2021 International Conference on Intelligent Technologies (CONIT)
Karnataka, India. June 25-27, 2021

WAMS based Thevenin Index for Voltage Stability Assessment of Power System Integrated with Wind Farm

Pradyumna Pradhan
Department of Electrical Engineering, Visvesvaraya National Institute of Technology,
Nagpur, India

Raju Chintakindi
Department of Electrical Engineering, Visvesvaraya National Institute of Technology,
Nagpur, India
rajuphdvnit@gmail.com

Arghya Mitra
Department of Electrical Engineering, Visvesvaraya National Institute of Technology,
Nagpur, India

2021 International Conference on Intelligent Technologies (CONIT) | 978-1-7281-8583-5/21/$31.00 ©2021 IEEE | DOI: 10.1109/CONIT51480.2021.9498450

***Abstract*— With the increase in the penetration of the renewable resources to the existing grid, the analysis of the effect of the penetration of such sources on the system stability is one of the major concerns. The impact of the significant penetration of the DFIG based wind farm on the voltage stability of the three machine power grid is addressed in this paper. The Voltage Stability Index (Local Thevenin Index-LTI) based on Wide Area Monitoring System is used here to evaluate the voltage stability of the overall power system. This index also helps to assess the optimal location for connecting the wind-farm to the current power grid from the point of view of system stability. The modelling and simulation of the work with WSCC multi-machine 9-bus power grid is carried out on the MATLAB-Simulink environment.**

Keywords*— multi-machine power system; WAMS; Local Thevenin Index; DFIG based Wind Farm; Voltage Stability.

I. INTRODUCTION

Exhausting fossil fuels and their environmental effects increase the integration of renewable sources, such as solar and wind energy, into the system [1]. Though being the oldest among all the renewable sources, wind energy is still gaining popularity as one of the fastest growing alternative resources in modern power sector. As these resources are unreliable and highly unpredictable in nature, this raises questions about the stability of the existing power grid. On the other hand, the increasing stress on power grid operators to use present infrastructure and services to the fullest possible degree, can lead to complications in terms of long-term voltage stability [2]. Grid operators are implementing real-time tools employing wide-area monitoring systems and smart automation (WAMSA) by using Phasor Measurement Unit Technology (PMUT) to enhance operational sensitivity [3]. WAMS is a collaborative technology for measuring the power system variables in real time, detecting stability of the system, associated vulnerabilities and helping to plan and operate with preventive measures. Synchrophasor processing unit is used to enhance grid efficiency by timely identification of faults and conditions of instability. The key advantage of the synchronized phasor measurement units is that it produces high precision time-tagged voltage and/or current phasors.

The wide-spread acceptance of PMUs has contributed to the growth of some voltage stability indices -VSIs that are used to track the system's long term voltage stability in online [4]. The VSI, calculated on a bus by measuring the Thevenin Equivalent from localized Synchrophasor measurements of voltage and current, is referred to as local Thevenin index (LTI) [5]. The consistency of the LTI computation has contributed towards its practical implementation and numerous regulation systems depending on the priorities of LTI such as to ensure that whether the system is far away from collapsing is studied in [6]. The benefit of such approaches is that they have a global view on the grid that existing technologies do not have. A potential purpose of a WAMS VSI could be to verify the LTI which is measured on the PMU. Since the LTI measured at the Synchrophasor unit is normally corrupted by the noise, it is impossible for the operator to initiate the control action in time as and when required. In order to correct this problem, wide area based Thevenin Index, known as sensitivity based Thevenin index (STI) was proposed to verify the LTI at the control room [5]. There are a few types of voltage stability indicators that can be derived from Synchrophasor samples, which primarily focus on VSI-dependent Thevenin equivalents. Such VSIs can be categorized into 2 types— a) Local Thevenin Index, only using local bus PMU recordings; and b) Central Thevenin Index, using WAMSA in a large area.

This paper analysed the effect of DFIG focused wind power integration to the power-system using LTI and thereby determining the best possible position of the point of connection of the wind farm from the point of view of overall system voltage stability condition. Here it is to be mentioned that, DFIG is one of the commonly used wind-energy machinery that can operate through both sub-synchronous and super-synchronous speed regions and extracts maximum available wind power. The impact on the system stability condition with the increase in the penetration of wind power is also studied with the help of the Local Thevenin Index.

This paper is arranged as follows: Section II defines primary knowledge about importance and use of the Real-time wide-area control framework using PMU technologies, Section III presents DFIG-based wind farm integration to power system, Section IV discusses the calculation of the Local Thevenin Index, Section V explores simulation and performance analysis and Section VI ends with the concluding remarks.

II. REAL-TIME WIDE AREA MONITORING SYATEM

The energy engineers are now focusing on the use of large-scale measurement instruments with advanced detection and protection technology. Thus, there is a constant increase of attention of more and more use of wide-area

monitoring technology in the present-day electrical grid. To track, monitor, and regulate the power networks in a wide geographical field, WAMSA integrates the roles of both traditional and recent metering instruments with the functionality of communications networks. One such example may be the infrastructural development by GE Power in the World's largest synchronized Indian Grid structure with 363 GW capability across a national wide-area control system [7].

In such system, information samples have been taken through PMUs from the AC waveform using an analog to a digital converter. Along with PMUs, the coordinated measuring device which contains Phasor Data Concentrators-PDCs, Utility Software and the support for its Communication Links. The Global Positioning System (GPS) device consists of a receiver circuit and an antenna that generates a 1PPS synchronized waveform. This signal has been utilized to rectify drifts in the oscillator of local-clock that maintains the fundamental time in the PMU [8]. Figure 1 illustrates the real time WAMSA PMUT by showing the location of PMUs in specified load areas, such as industry, farming and residential areas.

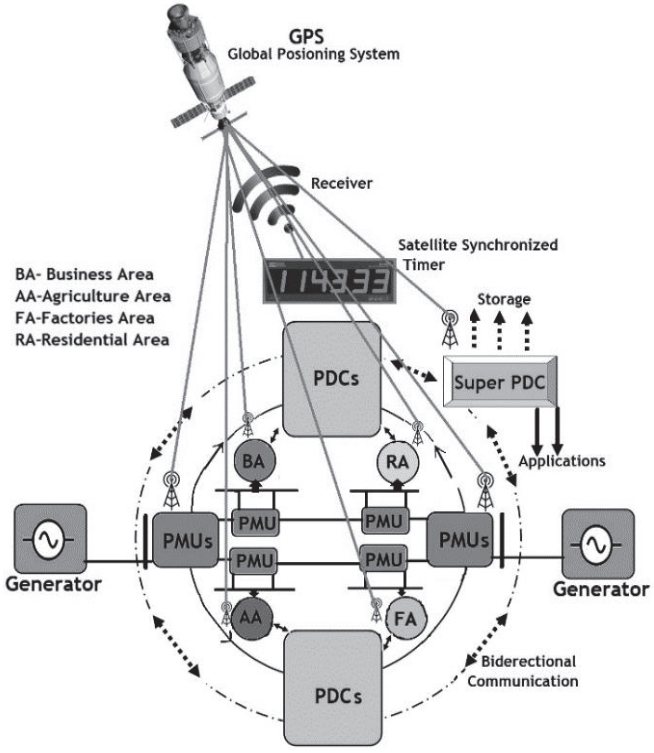

Fig. 1. Real-time wide-area monitoring system PMU technology [7]

III. DFIG BASED WIND FARM

These days, the assessment of voltage stability is a crucial subject in the power grid. Voltage stability can be impacted by a lot of elements, operating at different times. The effects of integrations of wind farm are undeniable in this respect. The penetration amount of wind power has been increased significantly in recent years. DFIGs are used as a wind generator in recent times in a power network. The exchange of reactive power with the grid so far be the main factor in relation to the voltage stability issue. Several methods have been developed associated to the DFIG reactive-power functionality curve in [9]. As an instance, the article [10] analyzed the DFIG reactive power capability through rotor side converter-RSC and grid side converter-GSC.

A DFIG is coupled to the system load bus by a dual-circuit line and a transformer [11]. The detailed description of the DFIG-connected grid is shown in Figure 2. It illustrates the connection of a DFIG based wind farm integrated to the 230kV utility bus by a transformer. Wind turbine is coupled to the DFIG by way of a gearbox through a gearbox ratio (n_s). P_s and Q_s are the real and reactive-power flow through stator. P_r and Q_r are the real and reactive power through the rotor, which is normally 30% of whole power.

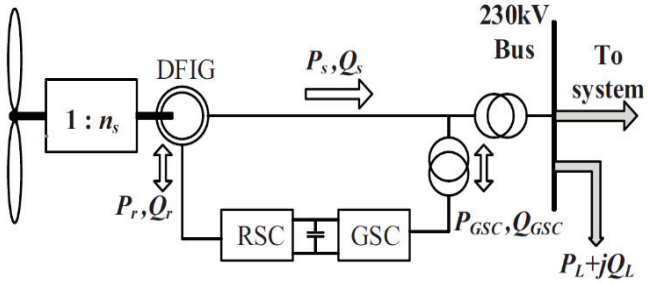

Fig. 2. Integrating the 100 MW DFIG focused wind farm to the multi-machine power grid

In this study, wind turbines and DFIG spinning masses are expressed by a 2 mass model as shown below [12]:

$$\frac{d\omega_r}{dt} = \frac{1}{2H_g}[K_{sh}\theta_{tw} + C_{sh}\omega_{elB}(\omega_t - \omega_r) - T_e] \quad (1)$$

$$\frac{d\theta_{tw}}{dt} = \omega_{elB}(\omega_t - \omega_r) \quad (2)$$

$$\frac{d\omega_t}{dt} = \frac{1}{2H_t}[T_m - K_{sh}\theta_{tw} - C_{sh}\omega_{elB}(\omega_t - \omega_r)] \quad (3)$$

For a stable and unsaturated state, the stator and rotor circuits are expressed by the equations given below [12]:

$$\frac{di_{ds}}{dt} = \frac{\omega_{elB}}{L'_s}\left[-\left(R_s + \frac{(L_{ss}-L'_s)}{T_r}\right)i_{ds} + L'_s i_{qs} - \frac{e'_q}{T_r} + \omega_r e'_d + K_{mrr}V_{dr} - V_{ds}\right] \quad (4)$$

$$\frac{di_{qs}}{dt} = \frac{\omega_{elB}}{L'_s}\left[-\left(R_s + \frac{(L_{ss}-L'_s)}{T_r}\right)i_{qs} + L'_s i_{ds} - \frac{e'_d}{T_r} + \omega_r e'_q + K_{mrr}V_{qr} - V_{qs}\right] \quad (5)$$

$$\frac{de'_d}{dt} = \omega_{elB}\left[\omega_s\frac{(L_{ss}-L'_s)}{T_r}i_{qs} - \frac{e'_d}{T_r} + \omega_s(\omega_s - \omega_r)\,e'_q - \omega_s K_{mrr}V_{qr}\right] \quad (6)$$

$$\frac{de'_q}{dt} = \omega_{elB}\left[-\omega_s\frac{(L_{ss}-L'_s)}{T_r}i_{ds} - \frac{e'_q}{T_r} - \omega_s(\omega_s - \omega_r)e'_d - \omega_s K_{mrr}V_{dr}\right] \quad (7)$$

Its torque formulas can be expressed as:

$$T_e = (e'_q i_{qs} + e'_d i_{ds})/\,\omega_s \quad (8)$$

$$T_m = \frac{0.5\rho\pi R^2 C_p(\lambda,\beta)v_w^3}{\omega_t}\left(\frac{1}{T_{mBase}}\right) \quad (9)$$

The total real and reactive power exchange with the power-grid by the wind generator can be given as:

$$P_{tot} = P_s + P_r = V_{ds}i_{ds} + V_{qs}i_{qs} + V_{dr}i_{dr} + V_{qr}i_{qr} \quad (10)$$

$$Q_{tot} = Q_s + Q_{GSC} = V_{qs}i_{ds} - V_{ds}i_{qs} \quad (11)$$

Where ω_{elB} = electrical base-speed; ω_s = synchronous speed; ω_r & ω_t = Electrical & mechanical speed of rotor; θ_{tw}= shaft torsional-angle; H_t & H_g= turbine & generator inertias respectively; K_{sh}= shaft-stiffness of the drive train; C_{sh}= damping coefficient of drive train; V_{qs}, V_{ds} & V_{qr}, V_{dr} = q-axis & d-axis voltages of stator and rotor respectively; i_{qs}, i_{ds} & i_{qr}, i_{dr} = q-axis & d-axis currents of stator and rotor respectively; e'_q & e'_d = equivalent voltage sources of q-axis & d-axis behind transient impedance respectively; L_m = mutual-inductance; L_{ss} & L_{rr} = stator & rotor inductances respectively; $L'_s = L_{ss} - \frac{{L_m}^2}{L_{rr}}$; R_s = stator resistances; $C_p(\lambda, \beta)$= coefficient of performance; v_w= wind speed; ρ=air density; R = wind turbine blade length; T_e = electrical torque; T_m = mechanical torque; Q_{GSC} = grid-side converter reactive power.

The stator windings of the DFIG are directly connected to the power grid, whereas the rotor is connected to the power grid via the AC/DC/AC converter. In this investigation, the speed of wind is kept fixed at 15 m/s. The scheme utilizes a speed controller to maintain the speed at 1.2 p.u. The DFIG is maintained the reactive power generated at zero.

IV. Computation of Local Thevenin Index (LTI)

LTI has been one of the voltage stability indicators that use WAMS computations to track the system's long-term voltage stability. It is measured on a load bus by calculating Thevenin equivalent employing localized PMU voltage and current quantities. The simplicity of LTI calculation makes it possible for its commercial execution. Besides, depending on the LTI importance, numerous control solutions have been introduced to make sure that the system is away from crashing [13]. The computation of the LTI is presented in [2] in a detailed manner.

The LTI at a load bus is described as the absolute value of the ratio between the approximate Thevenin impedance (Z_{ith}) to the Load-Impedance (Z_L) as presented in the equations (12) to (14). Thevenin impedance is been obtained by using two consecutive phasor measurements of voltage and current under the expectation that equivalent variables do not alter during the time interval in between the two measurements. The statement is true whenever the load increment ($\Delta\lambda$) between these two consecutive measurements is quite small.

$$Z_{thi} = \frac{V_i^{(2)} - V_i^{(1)}}{I_i^{(2)} - I_i^{(1)}} = \frac{\Delta V_i}{\Delta I_i} \quad (12)$$

$$Z_{Li} = \frac{V_i^{(1)}}{I_i^{(1)}} \quad (13)$$

$$LTI_i = \left|\frac{Z_{thi}}{Z_{Li}}\right| \quad (14)$$

Here $V_i^{(1)}$ & $I_i^{(1)}$ refers to the voltage and current phasor measured at the 1st instant i.e. initial steady-state condition, $V_i^{(2)}$ & $I_i^{(2)}$ refers to the voltage and current phasor measured at the 2nd instant i.e. after load increment and 'i' refers to the bus number.

As loading increases, the LTI value increases. At light load, the LTI value is close to 0 and at a heavy load, the LTI amount is close to 1. The LTI with a value less than 1 means that the system is at a desired operating state. Therefore, it can be stated that a system with lower LTI values is generally more stable than the system with higher LTI values.

V. Voltage Stability Assessment of the Power System using LTI

Figure 3 represents the diagram of the WSCC three-machine nine-bus system [14] which is considered for this study with a DFIG based wind farm integrated at all the three load buses of the power system, one at a time. A 100 MW wind power plant, consisting of sixty-seven 1.5 MW wind turbines, which are connected through a transformer to a 230 kV bus, is considered here.

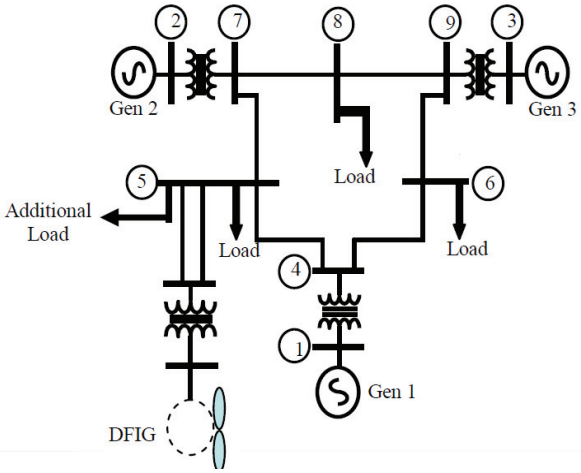

Fig. 3. Schematic representation of the WSCC three-machine nine-bus system with wind-farm integrated at bus 5

The wind-farm is integrated with the existing system to meet the additional load demand. The power produced by the wind farm is made equal to the additional load connected in the system. As both the additional load and wind farm are connected at the same bus, no change in the steady-state load-flow of the power network after integration of the wind-farm could be seen [12]. The output voltage and power waveforms of the 100 MW DFIG, when located on bus 8, are shown in Figure 4a and 4b. From the figures, it may be seen that the per unit value of the voltage at bus 8 is nearly at unity (as it was before the integration of the wind-farm) and the actual real power generation by the wind farm is maintained at 100 MW.

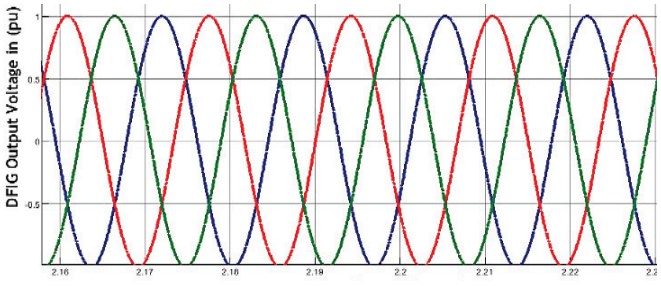

Fig. 4. (a). Output voltage waveforms of 100 MW DFIG on bus 8

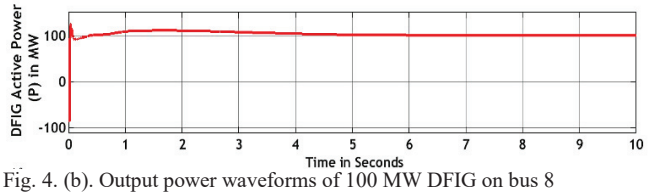

Fig. 4. (b). Output power waveforms of 100 MW DFIG on bus 8

The study aims at a) the selection of best location of the point of connection of the wind-farm from the voltage stability point of view and b) analysing the effect of increase in wind power penetration on the system voltage stability condition. Both the findings are based on the computed value of the LTI, as defined in Section IV.

A. The study of system voltage stability variation with varying wind farm locations:

The wind farm is established in an area where there is availability of ample wind speed. After selection of the wind farm area, one can determine the point of connection of the farm with the existing power system based on system stability condition, as system stability will vary with different point of connection. In the considered 9-bus system, the wind farm can be integrated at one of the three load buses i.e. bus 5, bus 6 & bus 8, considering that the average wind speed is high enough for the establishment of the wind farm. We must choose the best location among these 3 points from the stability point of view. This can be found out with the help of LTI.

PMU recordings of voltage-magnitude, phase angle, and frequency of bus 8 are shown in Figure 5. The LTI is calculated using (12)-(14) at all three load buses for different values of load increment Δλ (1% to 5%) for each location of wind farm integration. The results are shown in Table I.

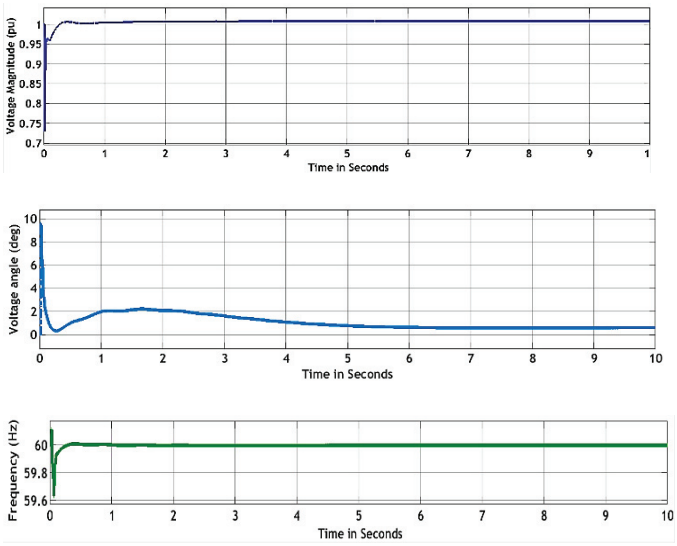

Fig. 5. PMU recordings of the voltage magnitude, phase angle, and the frequency of bus 8

TABLE I. VARIATION OF LTI FOR DIFFERENT WIND FARM LOCATIONS

Wind farm location	LTI with different Δλ					
	Bus \ Δλ	0.01	0.02	0.03	0.04	0.05
5	5	0.562	0.564	0.567	0.569	0.573
	6	0.511	0.514	0.516	0.520	0.525
	8	**0.483**	**0.485**	**0.488**	**0.493**	**0.496**
6	5	0.513	0.516	0.520	0.523	0.527
	6	0.448	0.450	0.453	0.457	0.461
	8	**0.417**	**0.420**	**0.424**	**0.426**	**0.431**
8	5	0.442	0.446	0.448	0.452	0.455
	6	0.372	0.374	0.377	0.380	0.382
	8	**0.343**	**0.345**	**0.348**	**0.350**	**0.353**

The best values of LTI, corresponding to each possible wind-farm positions and different load increaments, are presented in bold fonts

From Table I, it can be observed that the LTI values are varying with a change in the location of wind-farm integration, even for the same load increament. At first, the DFIG based wind-farm is integrated at bus 5 and LTI is calculated at all the three load buses for different load increment (Δλ is varying from 0.01 to 0.05 in steps of 0.01). The same thing is repeated for the wind-farm integration at bus 6 and bus 8. It is found that when the wind-farm is integrated at bus 8, we are getting lesser LTI values at all three load buses compared to the other two locations of wind farm integration. That means the system is relatively more stable when the wind-farm is integrated at bus 8. Therefore, bus 8 of the 9-bus system can be considered as the most preferred location for connection of wind-farm. To get a better view of the variations of LTI at different load buses when DFIG based wind farm is integrated at bus 5, 6 and 8, one by one, are shown in the Figures 6 to 8 respectively. The lowest height of the bars (yellow coloured bar in the figures) are corresponding to the LTI values calculated at bus 8 for any point of conncetion of wind farm. These values of LTI at bus 8 are different for different wind farm connection point as well as for different Δλ. To compare the LTI values at bus 8, Figure 9 is shown here. It may be observed from the Figure 9, that the least values of LTI for different Δλ is obtained when wind farm is integrated at bus 8. This ensures the best location of connection of wind-farm from the point of view of system voltage stability condition.

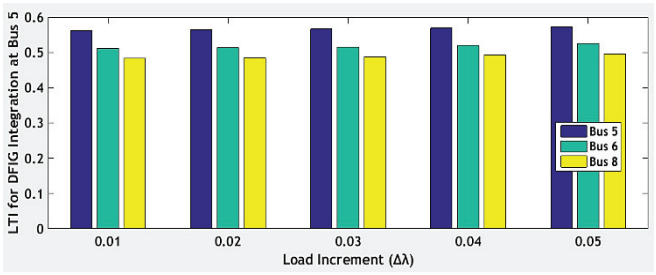

Fig. 6. LTI at load buses with DFIG Integrated at bus 5

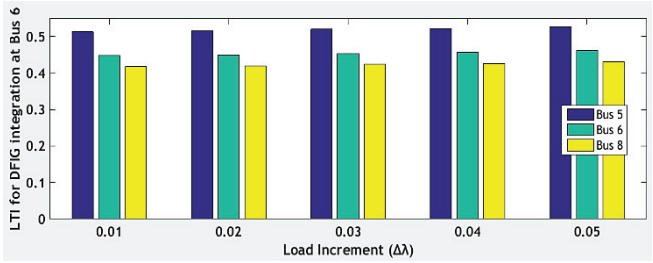

Fig. 7. LTI at load buses with DFIG Integrated at bus 6

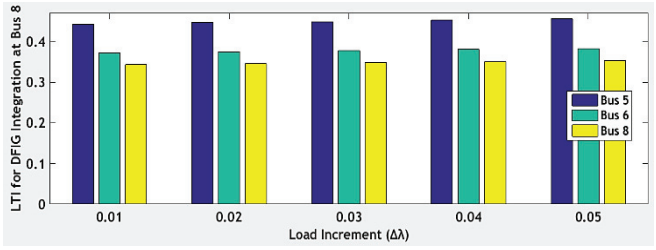

Fig. 8. LTI at load buses with DFIG Integrated at bus 8

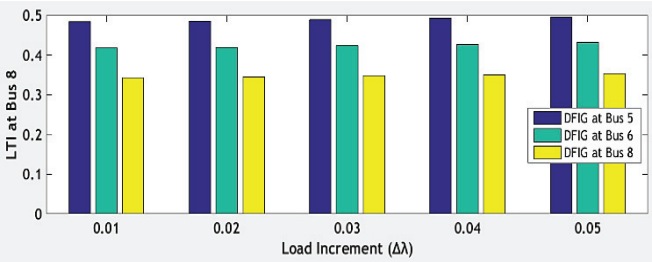

Fig. 9. LTI at bus 8 with DFIG Integrated at different locations

B. The effect of rise in wind power penetration level on the system voltage stability

The wind power penetration (%P) is the ratio of the aggregate wind power flowing into the power-system to the sum of all the existing loads ($\sum_{i=1}^{n} P_{Li}$) and the additional load at DFIG terminal bus, in the system [15]. It can be expressed as equation (15).

$$\%P = \frac{P_{dg}}{\sum_{i=1}^{n} P_{Li} + P_{dg}} * 100 \qquad (15)$$

Where P_{dg} in the denominator represents the additional load as the wind-power injected into the system is equal to the additional load.

For a wind-farm with a size of 100 MW integrated with the 9-bus system, the penetration level is found to be 24.1%. Here the wind power penetration level is varied and its impact on stability of the existing 9-bus system is studied with the help of LTI i.e. our focus is to see how the stability of the system is being affected by rise in the penetration of wind power.

The wind-farm is integrated at the most preferred location (bus 8) of the 9-bus system and the output power of DFIG is varied from 50 MW to 95 MW (corresponding penetration level is 13.7% to 23.2%). For each penetration level, the LTI is being calculated at all three load buses for 1% to 5% of load increment (Δλ) as before. The results are presented in Table II. It may be observed from Table II that the LTI values are varying with the rise in wind power penetration. As the wind farm output power is increased from 50 MW to 90 MW (corresponding rise in penetration from 13.7% to 22.2%), the LTI values of all three load buses start decreasing gradually. This indicates that the stability of the system is gradually increasing with the rise in wind-power penetration from 13.7% to 22.2%. When we increase the wind power beyond 90 MW, the LTI values of all three load buses start increasing. This indicates the system voltage stability is deteriorating with the increase in wind power beyond 90 MW (22.2% penetration). So, it can be said that the system stability is initially improved with the increase in the penetration up to 22.2% (P_{dg}= 90 MW) and beyond that, it starts deteriorating. Thus, from the system voltage stability point of view it is observed for the 9-bus system that the maximum wind-power penetration at bus-8 is 90 MW.

The effect on LTI, computed for bus 5, 6 and 8, due to increase in wind-power penetration, is presented in Figure 10 to Figure 12 respectively. It may be observed from the figures that for same amount of load increment, LTI varies with variation in wind power injection (i.e, the level of penetration of wind power). Further, it may be noticed from the figures that with rise in the wind-power injection, LTI decreases first and then starts increasing. It is clear from the figure that the LTI values are least corresponding to different Δλ, calculated at the three load buses when the penetration level is at 22.2% i.e, 90MW power generation by the wind farm.

TABLE II. EFFECT OF RISE IN WIND-POWER PENETRATION ON LTI

P_{dg} in MW (%P)	LTI with different Δλ					
	Δλ / Bus	0.01	0.02	0.03	0.04	0.05
50 (13.7)	5	0.478	0.482	0.487	0.493	0.499
	6	0.389	0.392	0.396	0.399	0.401
	8	0.347	0.350	0.354	0.356	0.359
70 (18.2)	5	0.466	0.470	0.472	0.475	0.478
	6	0.372	0.375	0.378	0.381	0.383
	8	0.334	0.336	0.339	0.342	0.345
90 (22.2)	5	0.423	0.425	0.428	0.431	0.433
	6	0.354	0.356	0.359	0.361	0.364
	8	0.327	0.329	0.332	0.335	0.339
91 (22.4)	5	0.426	0.429	0.433	0.436	0.440
	6	0.356	0.359	0.362	0.364	0.366
	8	0.330	0.332	0.336	0.339	0.343
93 (22.8)	5	0.429	0.431	0.434	0.437	0.441
	6	0.360	0.362	0.365	0.367	0.371
	8	0.333	0.337	0.340	0.342	0.347
95 (23.2)	5	0.431	0.434	0.436	0.439	0.442
	6	0.362	0.364	0.367	0.370	0.373
	8	0.335	0.339	0.343	0.346	0.349

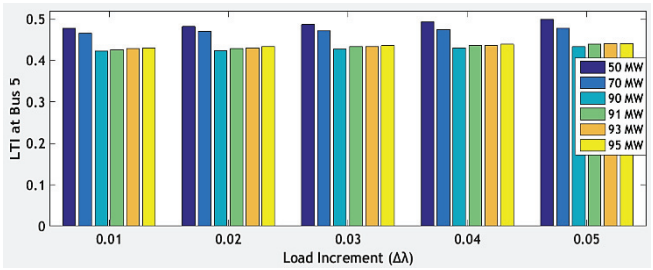

Fig. 10. LTI at bus 5 for various wind power penetration

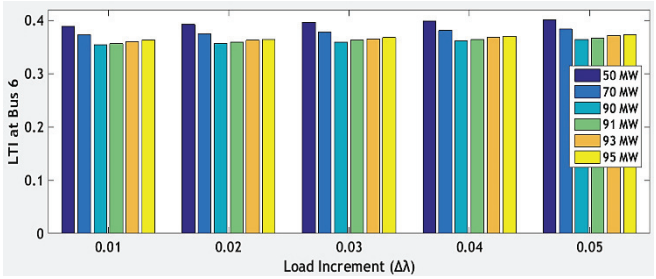

Fig. 11. LTI at bus 6 for various wind power penetration

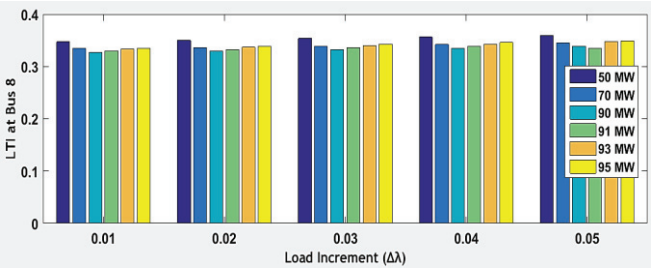

Fig. 12. LTI at bus 8 for various wind power penetration

VI. CONCLUSIONS

The voltage stability analysis has been performed for a multi machine power system (WSCC three-machine nine-bus system) integrated with a DFIG based wind farm using a WAMS based voltage stability index i.e. LTI. This index helps us to decide the optimal location for the connection of a 100 MW wind farm with the existing 9-bus system and it is found that bus 8 is the most suitable location as here we are getting least LTI values at all three load buses when compared to the other locations of wind farm integration. After deciding the best location for wind farm integration, the maximum wind power penetration at that location is also found with the help of the same index. It is observed that with the rise in wind-power penetration the LTI values computed at all three load buses decrease indicating improvement in system stability condition up to a certain level of penetration. There exists an optimum value of wind-power penetration exceeding which the LTI values of all the load buses start increasing, which indicates worsening of system stability. Thus, at this optimum penetration level, the system can attain its maximum stability when the DFIG based wind-farm is connected at the optimal location of the 9-bus system.

REFERENCES

[1] R. N. A. and S. P. Navghare, "An insight to distributed generation of electrical energy from various renewable sources," *International Conference on Energy Efficient Technologies for Sustainability (ICEETS)*, 2016, pp. 341–345.

[2] A. Reddy, R. Matavalam, and V. Ajjarapu, "Validation of the sensitivity based Thevenin Index on large systems," *IEEE Power and Energy Society General Meeting*, 2018, vol. 2018-January, no. 2, pp. 1–5.

[3] R. Chintakindi and A. Mitra, "PMU-based Real-time Load Balancing Strategy for Lights-out Case in India – A Case Study," *First IEEE International Conference on Smart Technologies for Power, Energy and Control*, 2020, no. September, pp. 5–10.

[4] M. Glavic and T. Van Cutsem, "A short survey of methods for voltage instability detection," in *IEEE Power and Energy Society General Meeting*, 2011, pp. 1-8.

[5] A. Reddy, R. Matavalam, S. Member, and V. Ajjarapu, "Sensitivity based Thevenin Index with Systematic Inclusion of Reactive Power Limits," *IEEE Trans. Power Syst.*, vol. 8950, no. c, pp. 1–10, 2017.

[6] M. Glavic et all, "See It Fast to Keep Calm: Real-Time Voltage Control Under Stressed Conditions," *IEEE Power Energy Mag.*, vol. 10, no. 4, pp. 43–55, 2012.

[7] R. Chintakindi and A. Mitra, "Execution of real-time wide area monitoring system with big data functions and practices," *PIICON 2020 - 9th IEEE Power India International Conference*, 2020.

[8] P. Brijesh, A. G. Lal, A. S. Manju, and A. Joseph, "Synchrophasors evaluation and applications," *2018 IEEE Texas Power and Energy Conference, TPEC 2018*, 2018, vol. 2018-February, pp. 1–6.

[9] C. Engelhardt, S., Erlich, I., Feltes, "Reactive power capability of wind turbines based on doubly fed induction generators," *IEEE Trans. Energy Convers*, vol. 26, pp. 364–372, 2011.

[10] J. . Kayikci, M., Milanovic, "Reactive power control strategies for DFIG based plants," *IEEE Trans. Energy Convers*, vol. 22, pp. 389–396, 2007.

[11] J. G. S. and W. L. Kling, "Impacts of distributed generation on power system transient stability," *EEE PES General Meeting*, pp. 2150–2155, 2002.

[12] A. Mitra and D. Chatterjee, "Active power control of dfig-based wind farm for improvement of transient stability of power systems," *IEEE Trans. Power Syst.*, vol. 31, no. 1, pp. 82–93, 2016.

[13] L. Chengxi, L.; Zhe, C.; Bak, C.L.; Zhou, "Adaptive voltage stability protection based on load identification using Phasor Measurement Units," *IEEE AP AP*, vol. 2, pp. 1246–1251, 2011.

[14] A. Mitra, "A New Sensitivity Based Approach to Study Impact of Wind Power Penetration on Transient Stability," *IEEE International Conference on Power Electronics, Drives and Energy Systems (PEDES)*, 2012.

[15] M. Fatnani and A. Mitra, "Small signal stability analysis of wind farm integrated multi-machine power system with distributed load," *8th International Conference on Power Systems: Transition towards Sustainable, Smart and Flexible Grids, ICPS 2019*, 2019, no. 1, pp. 6–10.